Computers and Concrete, *Vol. 11, No. 5 (2013) 411-440*
DOI: http://dx.doi.org/10.12989/cac.2013.11.5.411

Modelling of strains in reinforced concrete flexural members using alpha-stable distribution

K. Balaji Rao*, M.B. Anoop, K. Kesavan, S.R. Balasubramanian, K. Ravisankar and Nagesh R. Iyer

CSIR-Structural Engineering Research Centre, CSIR Campus Taramani, Chennai 600 113, India

(Received December 28, 2011, Revised October 5, 2012, Accepted October 29, 2012)

Abstract. Large fluctuations in surface strain at the level of steel are expected in reinforced concrete flexural members at a given stage of loading due to the emergent structure (emergence of new crack patterns). This has been identified in developing deterministic constitutive models for finite element applications in Ibrahimbegovic *et al.* (2010). The aim of this paper is to identify a suitable probability distribution for describing the large deviations at far from equilibrium points due to emergent structures, based on phenomenological, thermodynamic and statistical considerations. Motivated by the investigations reported by Prigogine (1978) and Rubi (2008), distributions with heavy tails (namely, alpha-stable distributions) are proposed for modeling the variations in strain in reinforced concrete flexural members to account for the large fluctuations. The applicability of alpha-stable distributions at or in the neighborhood of far from equilibrium points is examined based on the results obtained from carefully planned experimental investigations, on seven reinforced concrete flexural members. It is found that alpha-stable distribution performs better than normal distribution for modeling the observed surface strains in reinforced concrete flexural members at these points.

Keywords: reinforced concrete; surface strain; cracking; thermodynamics; alpha-stable distribution

1. Introduction

Strain in steel in reinforced concrete (RC) flexural members is used in the computation of crackwidth. The value of strain is affected by density of cracking. It is also noted that in the context of condition assessment of existing reinforced concrete structures, measured/computed surface strains play an important role. The focus in this paper is on identification of probabilistic models for describing the surface strain (i.e., the strain in the exterior side face of the beam) variations in reinforced concrete flexural members.

Based on an experimental investigation on RC flexural members, it has been reported that the measured strains at a given depth from extreme compression fibre, along the length of beam in pure flexure zone, exhibit large scatter (Desayi and Rao 1987). Also, it has been reported that the variation of average strain across the depth is linear. Assuming linear strain variation across the depth of beam and considering various basic quantities as random variables, a probabilistic

*Corresponding author, Chief Scientist, RRG, CSIR-SERC, E-mail: balajiserc1@yahoo.com

http://www.techno-press.org/?journal=cac&subpage=8 ISSN: 1598-8198 (Print), 1598-818X (Online)

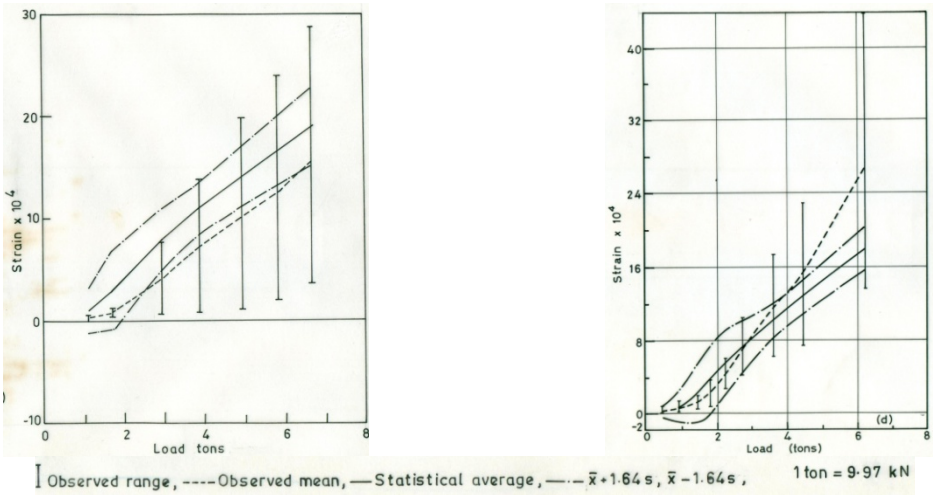

Fig. 1 Plots of load versus experimental surface strain, at the level of steel, for beams KB1 and KB2 at different stages of loading (from Desayi and Rao 1987)

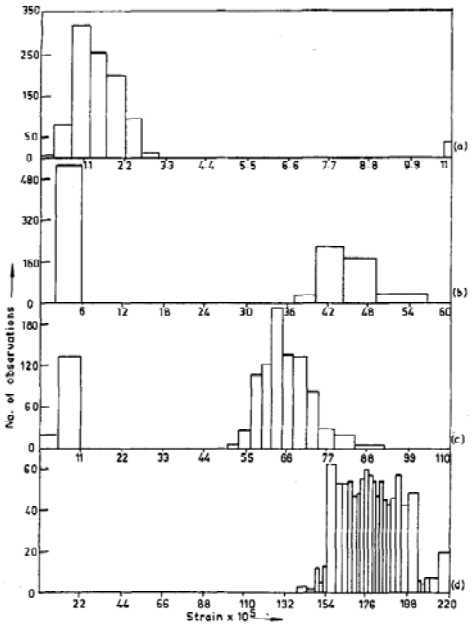

Fig. 2 Typical histograms of strains at the level of reinforcement for beam KB2: (a) at 1st stage of loading (applied load = 4.48 kN), (b) at 3rd stage of loading (applied load = 14.24 kN), (c) at 5th stage of loading (applied load = 22.25 kN) and (d) at 9th stage of loading (applied load = 65.73 kN) (from Desayi and Rao 1987)

analysis of average strain, at various stages of loading, was carried out using Monte Carlo simulation. From the results of simulation (Fig. 1), it has been found that the average strain at the level of reinforcement exhibits large scatter. The probabilistic mean overestimates the experimentally observed mean strains at lower stages of loading and underestimates the same at

Fig. 3 The RVEs in the constant moment zone of an RC beam

higher stages of loading. Also, it has been found that the (mean±1.64x standard deviation) limits does not enclose the observed range of strain at a given loading stage. Histogram of average strain distribution at the level of reinforcement (shown typically for the beam KB2 in Fig. 2) suggests that the distribution of average strain can be bi-modal and large scatter is expected in the prediction of average strain. These observations suggest that prediction of average strain itself is beset with large uncertainty. To predict/assess the condition of a reinforced concrete member prediction of extreme (largest) value of strain is important. Hence, it is important to model the strain as a random quantity taking into account the actual mechanism of cracking and by giving due consideration to the heterogeneity of concrete. As pointed out by Bazant and Oh (1983) "… This is clear even without experimental evidence, since structural analysis implies the hypothesis of smoothing of a heterogeneous material by an equivalent homogeneous continuum in which, if one uses the language of the statistical theory of random heterogeneous materials, the stresses and strains must be understood as the averages of the actual stresses and strains in the microstructure over the so-called representative volume whose size must be taken to be at least several times the size of the heterogeneities. …" The authors also give an idea about the size of the representative volume element (RVE) as 10 to 20 times the aggregate size. They have presented, by considering the energy criterion of fracture mechanics and strength criterion, equations for crack spacing and crackwidths in RC members. They attribute the possible variations in cracking to the random variations in fracture energy. From this study it is clear that when strain variation in the flexure zone is studied, the size of the RVE should be about 10 times the size of aggregate.

In the present investigation, the surface strains measured over a gauge length of 200 mm are considered for further analysis satisfying the requirement of RVE. Since the RVE is statistically homogeneous and all the RVEs (Fig. 3) in the flexure zone are subjected to same moment, these elements can be considered to be identical.

As suggested by Bazant and Oh (1983) and Balaji Rao and Appa Rao (1999), the RC beam undergoing flexural cracking can be considered as a parallel system wherein redistribution of stresses/strains are taking place. For such a system, Bazant (2005), using the fracture mechanics based size effect theory, has recently shown that the load (or stress) – displacement (or strain) curve would exhibit jumps. However, as pointed out by Bazant (2005), the size effect may not be significant in the presence of tension reinforcement. As discussed in this paper, even the load-displacement behaviour of RC beam would exhibit multiple jumps. The points where the jumps occur are the points of bifurcation (de Borst 1987, Bazant 2005, Bazant and Cedolin 2010, Ibrahimbigovic *et al.* 2010). It is known that at these points, the system which is undergoing flexural cracking would exhibit large fluctuations (Prigogine 1978). From the foregoing discussions it is felt that a heavy tailed distribution may be more appropriate to capture the large fluctuations in the concrete surface strains in reinforced concrete flexural members (at any given stage of loading, especially at the points at which an emergent crack structure forms).

Some observations:

- The RVEs located in the flexure zone of the RC member (Fig. 3) are subject to statistically similar stress/strain states. This implies that the random surface strains in the RVEs are identically distributed. While the stress/strain state in RVEs can be considered to be identical, they need not be considered to be statistically independent.
- From both the experimental and probabilistic analyses results, it is found that a random variable which exhibits large fluctuations would be preferred over those generally used (i.e., those with exponential decaying tails). Thus, it is desirable to use probability distributions that have power law decaying tails (since they have to capture large fluctuations expected to be attendant with bifurcation phenomenon).

An experimental program is taken up recently to check the validity of this inference. Four singly reinforced RC beams are tested under four point bending to obtain the concrete surface strain values in the flexure zone at CSIR-SERC. Salient details of experimental investigations are presented in this paper. An attempt is made to fit an alpha-stable distribution (which is known to have heavy tails) to the observed strains. To study further the efficacy of alpha-stable distribution for modelling the variations in strain in concrete at the level of reinforcement in RC flexural members, experimental investigations on three singly reinforced concrete beams presented by Desayi and Rao (1987, 1989) are also considered. Based on the results of statistical analyses it is inferred that the alpha-stable distribution is a good choice for modelling the surface strains in concrete, at the level of reinforcement, in RC flexural members.

2. Mechanism of cracking - A discussion on emergent structure

The strain in concrete in the tension zone of a RC flexural member depends on the level of cracking in the member. To understand the strain behaviour in the tension zone, it is important to know the mechanism of cracking in RC flexural member. The mechanism of cracking is described in several references (see for instance Bresler 1974, Park and Paulay 1975, Nilson and Winter 1986). Only a brief description of the same will be presented here.

When an under-reinforced concrete beam is subjected to monotonically increasing four-point bending (Fig. 4), the following points can be noted:

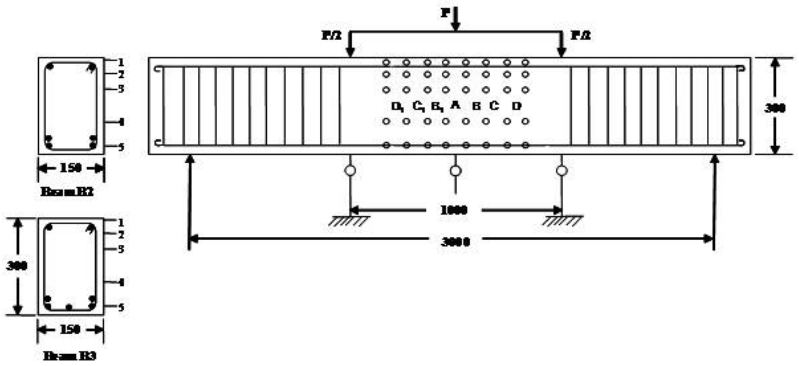

Fig. 4 Schematic representation of the test program for beams tested at CSIR-SERC (dimensions in mm)

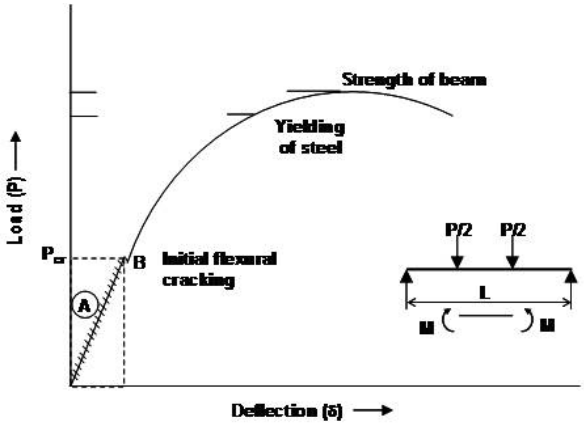

Fig. 5 Schematic load-deflection diagram of an under-reinforced concrete beam

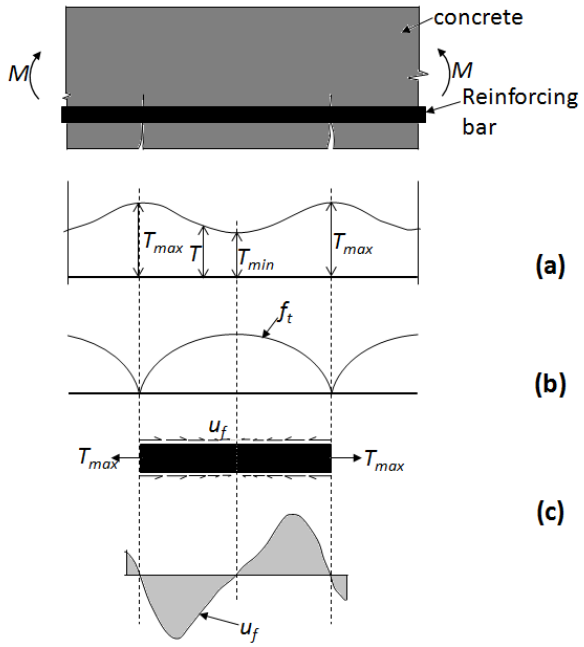

Fig. 6 Flexural cracking in reinforced concrete beam: (a) variation of tensile force in reinforcing bar, (b) variation of tensile stress in concrete, (c) variation of bond stress (based on Pillai and Menon 2009, MacGregor 1997)

(1) As long as the applied load is less than the first crack load of the beam, the tension forces are shared both by concrete and steel. The load-deflection curve will be essentially linear (portion A of Fig. 5). There will be internal micro-cracking of concrete present in the tension zone (Bresler 1974).
(2) When the applied load is equal to the first crack load of the beam, visible crack(s) appears on the surface of the beam and the flexure zone of the beam will be divided into number of sections as shown in Fig. 6. The formation of first set of cracks will be characterised by a sudden drop in load

(point B in Fig. 5). This occurs due to sudden loss of stiffness of the beam due to cracking. Typical variations of tensile force in steel, tensile stress in concrete and the bond stress in the flexure zone of the beam are shown in Fig. 6 (Pillai and Menon 2009, MacGregor 1997).
(3) With the increase of load, beyond the first crack load, redistribution of stresses take place between the cracked sections. New cracks may form in between the existing cracks and also the existing cracks may widen/lengthen. The formation of new cracks results in reduction in crack spacing. The process of formation of new cracks will continue until the bottom fibre stress in concrete cannot reach a value equal to the modulus of rupture. When this condition is reached, no more new cracks form and the existing cracks will widen/lengthen with the increase of load. Thus, the spacing of cracks remains the same and the corresponding crack spacing is called stabilised crack spacing.

From the above discussion, it is clear that the behaviour of RC flexural members under the external loading is quite complex. Also, it is clear that one of the outstanding features of the behaviour is the emergent structure at different stages of loading (in this paper, emergent (dissipative) structure refers to formation of new cracks and/or widening and lengthening of the existing cracks on the surface of the flexural member, in the constant bending moment zone), as the loading is increased monotonically. At a given stage of loading, the emergent structure is characterized by the crack length, crack spacing, crack width. Efforts have already been made to approximately account for these observations in the estimation of crack spacing and crack widths (ACI 2002, BS8110 1997, CEB 1990, Desayi and Ganesan 1985). From the equations proposed in these codes (not presented here), it can be noted that cracking in RC flexural members depend on cross-section dimensions of the beam, the material strengths and the reinforcement details.

Recently, efforts are being made to develop numerical models within the framework of finite element simulation for prediction of load-deformation behaviour of RC members. The formulation, as can be expected, should consider the fact that the RC beams would have both distributed and localized damage in coupled form and, also the bond-slip relation. Two types of models namely, one which is based on characteristic length and the other based on damage evolution have been proposed (Bazant and Oh 1983, Sluys and de Borst 1996, Dominguez *et al.* 2005, Ibrahimbegovic *et al.* 2010). The latter type of models recognises that there can be strong discontinuities in the displacement field at the points of bifurcation. From a brief review of these models, it is noted that when fracture energy based models are used in FEM of RC members, the gradient crack model proposed by Sluys and de Borst (1996) with a refined bond-slip model can be used. However, it is felt that the constitutive relations proposed by Dominguez *et al.* (2005) are best suited since they are based on strong displacement field discontinuity hypothesis. This type of model is recommended in probabilistic simulation. In this paper, attempt is made to first suggest a probabilistic model for surface strains based on phenomenological considerations and then examine its applicability based on experimental observations only. And, no FE modeling and simulations are attempted. These studies are being continued at CSIR-SERC.

3. Probabilistic model for surface strains in RC members

It is known that when the principles of thermodynamics are applied to describe the cracking phenomenon of RC beams, the stage at which emergent structure forms corresponds to a transient non-equilibrium condition and subsequent formation of a meta-stable state(s) (de Borst 1987, Balaji Rao 2009). See Appendix I for a brief description on the evolution of a non-equilibrium

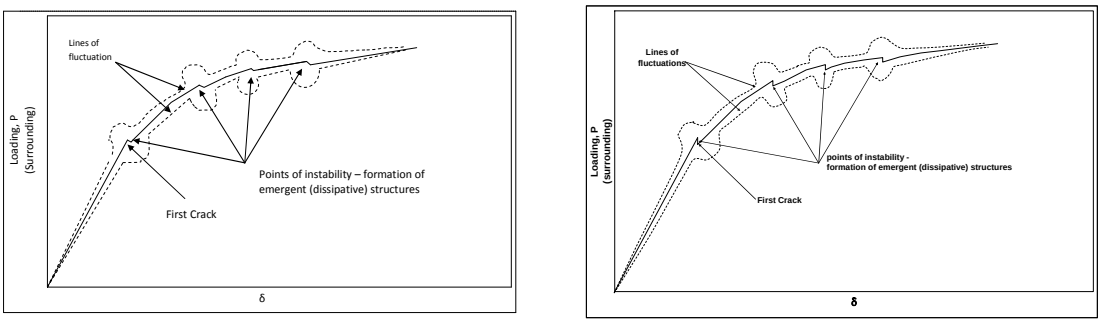

(a) (b)

Fig. 7 Schematic of response evolution with loading showing formation of emergent (dissipative) structures (a) gravity-load testing and (b) displacement controlled testing

thermodynamic system (see de Groot and Mazur 1984). The loading drops at the incipience of an emergent structure marking the non-equilibrium thermodynamic state. This is transient non-equilibrium thermodynamic state because, further increase in load (from the load level to which it has reduced) can be achieved only with the increase in deflection of the beam. Once a particular stabilised crack pattern has formed, the beam will take further loading, which defines local equilibrium state with respect to cracking. This crack pattern will correspond to a meta-stable equilibrium state. The response evolution at and around the point of instability (such as the point 'B' which is in non-equilibrium state) is governed more by the fluctuations than the mean. Hence, mean field theory cannot be used to predict the behaviour around this point. However, beyond the unstable point, the response evolution can be predicted using mean field theory till another non-equilibrium point is reached (if at all possible). This behaviour is depicted in Fig. 7 for both gravity-load testing and displacement controlled testing. However, in this paper, only the former is considered.

It has been pointed out in the literature (Prigogine 1968, de Borst 1987, Balaji Rao 2009) that the application of thermodynamic principles to irreversible processes (which is typically the case of cracking in reinforced concrete beams) would result in large fluctuation and formation of a new (emergent) structure at the points of instability. This is due to the presence of wild randomness, which can simply be elucidated as follows: an environment in which a single observation or a particular number can impact the total in a disproportionate way (Mandelbrot and Taleb 2006). The traditional Gaussian way of looking at the world begins by focusing on the ordinary, and then deals with exceptions or so-called outliers as ancillaries. A second way, which takes the so-called exceptional as a starting point and deals with the ordinary in a subordinate manner - simply because that "ordinary" is less consequential. These two models correspond to two mutually exclusive types of randomness: mild or Gaussian on the one hand, and wild, fractal or "scalable power laws" on the other. To characterise and quantify the fluctuations at the points of instability, a distribution with heavy tails is to be used.

4. Justification for use of alpha-stable distributions

One of the significant factors affecting the surface strains in concrete is the cracking in concrete. Recent developments in NDE techniques (viz. AE, GPR and other sensors) have made it possible

to study the cracking process in concrete at micro-scale levels. Colombo *et al.* (2003), with a view to identify the damage due to cracking using acoustic emission (AE) technique, conducted experimental investigations on a RC beam subjected to cyclic loading. The beam was simply supported and was subjected to two-point bending. For each loading cycle, the peak load was increased from that in the previous cycle. After the end of last (tenth) loading cycle, the RC beam was found to be severely damaged. The AE data recorded at each loading cycle was analysed to determine the b-value (the b-value is the negative gradient of the log-linear AE frequency/amplitude plot). Colombo *et al.* (2003) stated that the changes in b-value can be related to the different stages of crack growth in the RC beam. At initial stages of loading, microcracks are dominant and the macrocracks would start to appear. The b-value corresponding to this phase is found to be greater than 1.7. In the next phase, the macrocracks would be uniformly distributed along the beam and no new macrocraks would form. The b-value corresponding to this phase is found to be between 1.2 and 1.7. In the final phase, the macrocracks were found to be opening up, as the beam is failing, and the b-value corresponding to this phase was found to be between 1.0 and 1.2. These studies thus help in locating- and assessment (qualitative) of- the damage. Carpinteri *et al.* (2009), based on both in-situ field test on RC member and laboratory tests on concrete specimens, have shown that the b-value can be linked to the value of exponent of the power law form for the tail portion of the probability distribution of crack size, and that the value of exponent of the power law can be interpreted as the fractal dimension of the damage domain. Therefore, the random variables associated with crack size in RC flexural beams should have a form consistent with the power law distribution (thus, may not have finite moments). By viewing the surface strains as a result of the indicated microscopic phenomena (such as bond-slip between steel and concrete, micro-cracking in concrete), the limiting distribution (attractor) is to be an alpha-stable distribution, knowing that the microscopic components may have power law distributions.

4.1 Thermodynamics considerations

The information presented in this section is based on the concepts presented by Prigogine (1978). An attempt has been made to interpret these concepts to the phenomenon of cracking in reinforced concrete flexural members.

According to Prigogine (1978), the concept of time in the case irreversible thermodynamic systems can be replaced by associating or suitably defining a variable associated with the phenomenon of formation of dissipative structures. Through suitable thermodynamic formulations, he has addressed the problem associated with these systems both at macroscopic and microscopic levels simultaneously. However, the use of Helmoltz free energy in the thermodynamic formulations is questioned since non-equilibrium can be source of order. Therefore, in order to formulate the problem of cracking which forms dissipative structures, the concept of open system needs to be adopted. The two components, namely, internal and external, are body of the material containing micro-cracks and the fictitious system containing localized macro-cracks which dissipate energy through mainly surface energy. These two systems are coupled and there exists a boundary between them. In this way, the thermodynamic formulations with strong discontinuity seem to show promise (Dominguez *et al.* 2005).

The second law of thermodynamics suggests that the change in entropy is equal to or greater than zero. For a closed system, the entropy production is through the irreversible damage and sets one-sidedness of time. The positive sidedness of time is associated with increase of entropy. If

entropy remains constant, time will not increase! This may be a problem with thermodynamics of closed systems. Hence, more often thermodynamics principles are applied to describe the systems near the equilibrium. To extend the thermodynamics to the non-equilibrium processes, an explicit expression for entropy production is required. Progress has been achieved along this line by supposing that even outside equilibrium, entropy depends only on the same variables as at equilibrium. This assumption leads to "local" equilibrium, and enables one to use the formulations similar to equilibrium thermodynamics. Local equilibrium requires that

$$\frac{d_i S}{dt} = \sum_{\rho:} J_\rho X_\rho \geq 0 \tag{1}$$

The left hand side of Eq. (1) gives the rate of production of internal entropy by the system due to various irreversible processes (ρ) at a macroscopic level. $J\rho$ and $X\rho$ are rate of entropy production by individual irreversible process ρ, and the driving force of the process ρ. This is the basic formula of macroscopic thermodynamics of irreversible process. At thermodynamic equilibrium, we have simultaneously for all irreversible processes

$$J_\rho = 0; X_\rho = 0 \tag{2}$$

It is therefore natural to assume that at least near the equilibrium linear homogeneous relations between flows and forces. The assumption of thermodynamic local equilibrium for non-equilibrium systems and application of above approach, at a macro scale, allows the use of empirical laws such as Fourier's law, and Fick's second law of diffusion to various phenomenon under consideration. It may be noted that we have not yet included the complex interaction that may takes place between the irreversible damage processes that are producing the entropy. The answer lies in the linearization of the system at least near the "local" equilibrium. This assumption enables the principle of superposition which is central to the local equilibrium thermodynamics and enables us to determine the rates of flow (flux) of a given irreversible process, taking into account the interactions among various irreversible processes contributing to the macroscopic equilibrium, using phenomenological coefficients ($L_{pp'}$) from the following relation

$$J_\rho = \sum_{\rho'} L_{\rho\rho'} X_{\rho'} \tag{3}$$

Linear thermodynamics of irreversible processes is dominated by two important results, namely, Onsager reciprocity relations and the principle of minimum entropy production at or very near the local equilibrium point. The Onsager reciprocity relation is given by

$$L_{\rho\rho'} = L_{\rho'\rho} \tag{4}$$

When the flow J_ρ,, the flow corresponding to irreversible process ρ, is influenced by the force $X_{\rho'}$ of irreversible process ρ', then the flow $J_{\rho'}$ is also influenced by the force X_ρ through the same phenomenological coefficient. It may be seen that the Onsager's reciprocity relation is similar to the Betti's theorem in structural engineering.

The two central concepts for establishing the "local" equilibrium dynamics of the irreversible thermodynamic open systems have been explained above. The theorem dealing with minimum

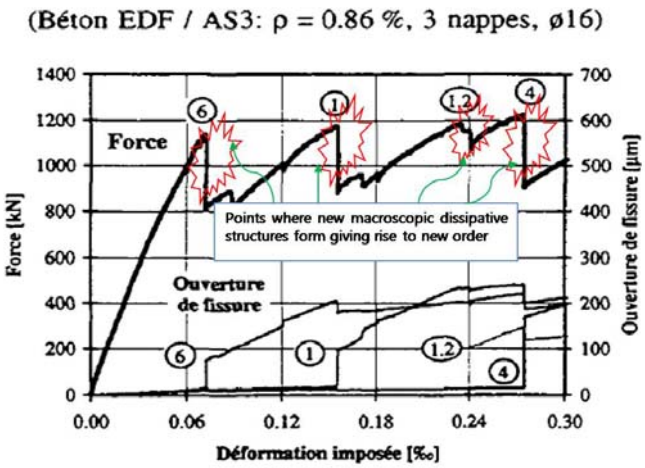

Fig. 8 Force-deformation relation of an RC member subjected to axial tension (Ibrahimbegovic *et al. 2010*)

internal entropy production is very significant since it gives some kind of 'inertial' property to the nonequilibrium system near the local equilibrium point. When given boundary conditions prevent the system from reaching thermodynamic equilibrium (that is zero entropy production) the system settles down to the state of 'least dissipation'. It is to be noted that for far-from equilibrium points the thermodynamic behavior could be quite different. It has been proved now that the behavior of the system can be opposite of minimum entropy production. In fact, the state of non-equilibrium (wherein there can be production of internal entropy) may be source of order at a macro-scale.

It is interesting to note that Boltzmann's order principle as expressed by canonical distribution assign almost zero probability to the occurrence of Benard convection. Whenever new coherent states occur far from equilibrium, the very concept of probability, as implied in the counting of number of complexions, breaks down. In the case of Benard's convection, above a critical temperature small convection currents, appearing as fluctuations, get amplified and give rise to macroscopic current. A new supermolecular order appears which corresponds basically to a giant fluctuation stabilized by exchanges of energy with the outside world. This is the order characterized by the dissipative structures.

The experimentally obtained force–displacement response and crackwidths for an RC member undergoing displacement-controlled traction test are shown in Fig. 8. The load-deformation process in RC member under monotonically increasing loads involves irreversible damage process. But, as mentioned earlier, the cracking process needs to be considered as both closed and open thermodynamic system forming dissipative structures at critical points (such as points 6, 1, 1.2, 4 in Fig. 8). But for points at which loading drops, which are points of non-equilibrium and far from equilibrium, local equilibrium can be obtained and we can define the local stationary states of the system (this enables us to use Onsager's reciprocity relation and the minimum dissipation theorem). At the points where it has been marked as red balloons, new emergent dissipative structures form (i.e., new macro-cracks form on the surface of the beam) indicating that these irreversible states correspond to the points far from equilibrium condition (something similar to Benard's convection presented by Prigogine (1978)). And, it is at these points the surface strains show large variability and the applicability of probability distribution with exponential tails is

questionable. The need for the use of alpha-stable distribution at points far from equlibrium due to formation of dissipative structures (thus bringing the order) is clearly brought out in thermodynamic framework by Rubi (2008).

Prigogine has shown that near critical points as well as near the co-existence curve (shown in red balloons in Fig. 8) the law of large numbers as expressed the expression

$$\frac{\left\langle (\delta X)^2 \right\rangle}{\mathrm{V}} \sim \text{finite for } \mathrm{V} \to \infty \tag{5}$$

(where X is a random variable representing an extensive quantity of thermodynamics), breaks down, as $\left\langle (\delta X)^2 \right\rangle$ becomes proportional to a higher power of volume. Prigogine (1978) has shown that near the critical points, probability distributions with long range memory would be needed. It is in this context, alpha-stable distributions are proposed to describe the fluctuations in surface strains near the critical points in the flexural members.

As mentioned earlier, one of the outstanding features of the behaviour of RC flexural beams under the external loading is the emergent structure at different stages of loading. The loading drops at the incipience of an emergent structure marking the non-equilibrium thermodynamic state. This is transient non-equilibrium thermodynamic state because, further increase in load (from the load level to which it has reduced) can be achieved only with the increase in deflection of the beam. Once a particular stabilised crack pattern has formed, the beam will take further loading, which defines local equilibrium state with respect to cracking. This crack pattern will correspond to a meta-stable equilibrium state. The response evolution at and around the point of instability is governed more by the fluctuations than the mean. Hence, to characterise and quantify the fluctuations at these points, a distribution with heavy tails is to be used.

4.2 Statistical arguments

For normal distribution 99.74% of total probability content is contained within three times standard deviation about the mean, thus giving low values of probability to the tail regions. The symmetric nature of normal distribution also restricts its applicability to phenomena exhibiting small skewness. Hence, there is a need to use distributions with heavy tails to model the strains showing large fluctuations and to estimate the extreme values. While there are different heavy-tailed alternatives to normal distribution, like alpha-stable distribution, Student's t-distribution, hyperbolic distribution, the use of alpha-stable distribution is supported by the generalized central limit theorem (see Appendix II). The use of alpha-stable distribution over normal distribution has found applications in different areas (see Nolan 2009, Yang 2009). The use of alpha-stable distribution for modeling the strain in RC flexural beams at a given loading stage is explored in the present study to account for the large fluctuations.

From the above, it is clear that to predict the extreme value of strains developed in RC flexural beams, at any stage of loading, a probability distribution with power-law tails should be used.

5. Alpha-stable distribution

The alpha-stable distribution is described by its characteristic function (an explicit expression

for probability density function generally does not exist) given by

$$L_{\alpha,\beta}(t) = E\left[\exp(itX)\right] = \begin{cases} \exp\left\{-c^{\alpha}|t|^{\alpha}\left[1 - i\beta\,\mathrm{sgn}(t)\tan\left(\frac{\pi\alpha}{2}\right)\right] + i\delta t\right\}; \text{ for } \alpha \neq 1 \\ \exp\left\{-c|t|\left[1 + i\beta\,\mathrm{sgn}(t)\frac{2}{\pi}\ln|t|\right] + i\delta t\right\}; \text{ for } \alpha = 1 \end{cases} \quad (6)$$

where X is the random variable, i is the imaginary unit, t is the argument of the characteristic function ($t \in \Re$), $E\left[\exp(itX)\right]$ denotes the expected value of $\exp(itX)$, α is an index of stability or characteristic exponent ($\alpha \in (0,2]$), β is the skewness parameter ($\beta \in [-1,1]$), c is a scale parameter ($c > 0$), δ is a location parameter ($\delta \in \Re$), ln denotes the natural logarithm and sgn(t) is a logical function which takes values -1, 0, 1 for t < 0, t = 0 and t >0, respectively. It may be noted that the skewness parameter β is not the same as the classical skewness parameter (Nolan 2009), since for non-Gaussian stable distributions, the moments do not exist. In the case of the alpha-stable distribution, the values of β indicate whether the distribution is right-skewed ($\beta > 0$), left-skewed ($\beta < 0$) or symmetric ($\beta = 0$). As α approaches 2, β loses its effect and the distribution approaches the normal distribution regardless of β (Borak *et al.* 2005). A stable probability density function (PDF) is symmetrical when β=0. The distribution is called standard stable when c =1 and δ=0. The general PDF of the stable distribution can be standardized such that (Belov 2005)

$$p(x,\alpha,\beta,c,\delta) = \frac{1}{c}\,p\left(\frac{(x-\delta)}{c},\alpha,\beta,1,0\right) \quad (7)$$

5.1 Estimation of parameters of alpha-stable distribution

Different methods have been proposed in literature for the estimations of the parameters α, β, c and δ of the alpha-stable distribution. Fama and Roll (1971) suggested a quantile-based method for estimation of characteristic exponent and scale parameter of symmetric alpha-stable distributions with δ = 0. However, this method is applicable only for distributions with α>1. This method has been modified by McCulloch (1986) to include even non-symmetric distributions with α in the range [0.6, 2.0]. Koutrouvelis (1980) proposed a characteristic function-based method involving an iterative regression procedure for estimation of the parameters of the alpha-stable distribution. Kogon and Williams (1995) improved this method by eliminating the iterative procedure and simplifying the regression. Ma and Nikias (1995) and Tsihrintzis and Nikias (1996) proposed the use of fractional lower order moments (FLOMs) for estimating the parameters of symmetric alpha-stable distributions. Bates and McLaughlin (2000) studied the performances of the methods proposed by McCulloch (1986), Kogon and Williams (1995), Ma and Nikias (1995) and Tsihrintzis and Nikias (1996) using two real data sets. They found that there are marked differences between the results obtained using the different methods. Nolan (2001) presented a maximum likelihood estimator (MLE) for estimating the parameters of alpha-stable distribution. However, to the authors' knowledge, the strong consistency of the MLE for alpha-stable distributions is yet to be proved. In the present study, the parameters α, β, c and δ of the alpha-stable distribution are estimated using an optimization procedure by minimizing the sum of squares of the difference between the observed cumulative distribution function (empirical

distribution function) and the cumulative distribution function (CDF) of the alpha-stable distribution (Maymon *et al.* 2000).

In the present study, the parameters α, β, c and δ of the alpha-stable distribution are estimated using an optimization procedure by minimizing the sum of squares of the difference between the observed cumulative distribution function (empirical distribution function) and the cumulative distribution function (CDF) of the alpha-stable distribution. The procedure used is as follows

1. Given the N ordered observed data points $x1$, $x2$, $x3$, …,xN, define the empirical distribution function as

$$E_N(i) = \frac{n(i)}{N+1} \tag{8}$$

where $n(i)$ is the number of data points less than or equal to xi, and xi are ordered from smallest to largest value.

2. Define the objective function as

$$Z = \sum_{i=1}^{N} \left(E_N(i) - \widetilde{F}_{\alpha S}(x_i; \alpha, \beta, c, \delta) \right)^2 \tag{9}$$

where $\widetilde{F}_{\alpha S}(x_i; \alpha, \beta, c, \delta)$ is the CDF of the alpha-stable distribution. ~ denotes the fact that the form of distribution function is generally not available and has to be approximated numerically.

3. Determine α, β, c and δ by minimizing Z subject to the constraints $0 < \alpha \le 2$, $-1 \le \beta \le 1$ and $c > 0$. In the present study, the minimization is carried out using the constrained nonlinear optimization function available in the software MATLAB. The CDF of the alpha-stable distribution, $\widetilde{F}_{\alpha S}(x_i; \alpha, \beta, c, \delta)$, is computed by numerical integration (Nolan 1997) using the MATLAB function developed by Veillette (2011).

The methodology used, in the present study, for probabilistic modeling of observed surface strains in RC flexural beams is illustrated in Fig. 9.

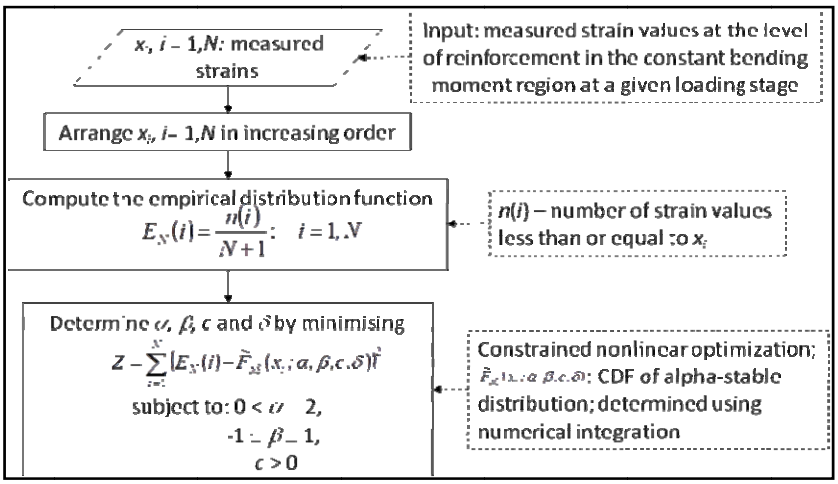

Fig. 9 Methodology for probabilistic modelling of observed surface streins in reinforced concrete flexural members

6. Applicability of alpha-stable distribution

In this section, an attempt is made to examine the applicability of alpha-stable distribution to model the surface strains in RC flexural members based on experimental observations. The data on variation of strain with loading for RC beams used in this study is based on the experimental investigations carried out at CSIR-SERC, Chennai, India and the experimental investigations reported by Desayi and Rao (1987, 1989). This data is used in the present study, since strain measurements over the entire constant bending moment region along the span at different positions for different loading stages (upto almost close to ultimate) for RC flexural beams have been taken and reported, which will be useful for studying the usefulness of alpha-stable distribution for modeling the variations in measured strain. Availability of such extensive data is scanty in literature. Salient information regarding the experimental investigations is given below.

7. Details of experimental investigations

7.1 Experimental investigations carried out at CSIR-SERC

Two sets of beams (with two beams in each set) of similar cross-sectional dimensions of 150 mm x 300 mm and 3.6 m long were cast and tested in four-point bending over an effective span of

Table 1 Details of beams tested at CSIR-SERC

SET	No. of Specimens	Grade of Concrete	Main reinforcement*	Stirrups	Hanger bars	Clear cover (mm)
B2	2 (B2-1, B2-2)	M30	2, 10mm dia. 2, 12mm dia.	6mm dia @ 140mm c/c	2, 6mm dia	25
B3	2 (B3-1, B3-2)	M30	5, 10mm dia.			

(Note: * - The main reinforcement is selected so as to have approximately the same cross-sectional area of reinforcement for all the beams)

Table 2 Properties of beams tested at CSIR-SERC

Beam	d_1* (mm)	d_2* (mm)	Effective depth (d) (mm)	A_{st1}** (mm^2)	A_{st2}** (mm^2)	A_{st} (mm^2)	150 mm concrete cube compressive strength (MPa)***	Split tensile strength (MPa)***	Cracking load (kN)**	Ultimate load (kN)***
B2-1	227.6	263.5	249.1	139.94	208.85	348.79	45.39	1.91	21.10#	77.74
B2-2	227.6	263.2	249.0	144.36	217.56	361.92	50.52	1.76	21.10#	82.89
B3-1	229.3	264.3	250.5	144.0	219.66	363.66	50.30	1.85	21.10#	83.88
B3-2	229.5	264.5	250.4	146.30	217.72	364.01	43.03	1.90	21.10#	82.80

(Note: span (l) = 3000 mm, breadth (b) =150 mm and depth (D) = 300 mm for all the beams; * - d_1 and d_2 are the depth from top of the beam to the centre of the main reinforcing bars in the top layer and bottom layer, respectively; ** - based on measured diameters of the reinforcing bars; *** - obtained from experimental investigations; # - cracking is initiated between applied loads of 14.72 kN and 27.47 kN and the average of these two loads is reported here as the cracking load)

3.0 m. Stirrups of 6 mm diameter were provided in the combined bending and shear zone to avoid shear failure, and no stirrups were provided in the constant bending moment zone. Details and properties of the beams are given in Tables 1 and 2. In the constant bending moment zone of the beams (i.e., 1m long), seven sections (denoted as D_1, C_1, B_1, A, B, C and D on the north face and, D', C', B', A', B_1', C_1' and D_1' on the south face) were identified, with each section having a gauge length 100 mm (see Fig. 4).

In each section, demec points were fixed at five different positions across the depth on both the faces of the beam (north face and south face). As can be seen from Fig. 4, position 1 corresponds almost to the extreme compression fibre for all beams; and position 5 corresponds to position of bottom layer of main reinforcing bars. The beams were tested in four-point loading. To measure the surface strains at different positions, a Pfender gauge with least count 1/1000 mm and gage length of 100.1 mm was used. While the strains were also monitored using electrical strain gages embedded on the reinforcement, for health assessment and maintenance decision making, strain readings from surface mounted strain gages are more useful than point estimates of strain. Hence, the present study focuses on modelling the surface strains at different stages of loading. The loads applied on the beams at different loading stages are given in Table 4.

At each loading stage, the strain readings are taken only after the applied load is stabilised, i.e., the loading has been increased to its original value after the drop in loading due to the incipience of emergent structure. The crack pattern observed for beams B2-1 and B3-1 at different stages of loading are shown in Fig. 10. The formation of emergent structure with loading is evident from these figures.

Table 3 Details of beams presented in Desayi and Rao (1987, 1989)

Beam	Effective depth (d) (mm)	A_{st} (mm^2)	150 mm concrete cube compressive strength (MPa)	Modulus of rupture (MPa)*	Cracking load (kN)*	Ultimate load (kN)*
KB1	311.0	402.123	33.078	4.036	23.549	95.389
KB2	305.4	437.929	40.417	3.578	14.014	104.653
KB3	303.5	529.327	22.508	2.950	8.899	84.291

(Note: span (l) = 4200 mm, breadth (b) =200 mm and depth (D) = 350 mm for all three beams
* - obtained from experimental investigations)

Table 4 Loads applied on the beams at different stages of loading

Loading Stage	Load Applied (kN)						
	B2-1	B2-2	B3-1	B3-2	KB1	KB2	KB3
1	0.98	0.98	0.98	0.98	10.52	4.48	8.90
2	2.45	2.45	2.45	2.45	16.61	8.90	17.80
3	4.91	7.36	4.91	4.91	28.99	14.24	26.67
4	7.36	14.72	7.36	7.36	38.28	17.80	39.78
5	14.72	27.47	14.72	14.72	48.95	22.25	52.97
6	27.47	40.22	27.47	27.47	57.37	26.67	70.90
7	40.22	52.97	40.22	40.22	65.66	35.42	-
8	52.97	58.86	52.97	52.97	-	44.16	-
9	-	63.77	65.73	65.73	-	57.44	-
10	-	68.67	-	-	-	-	-

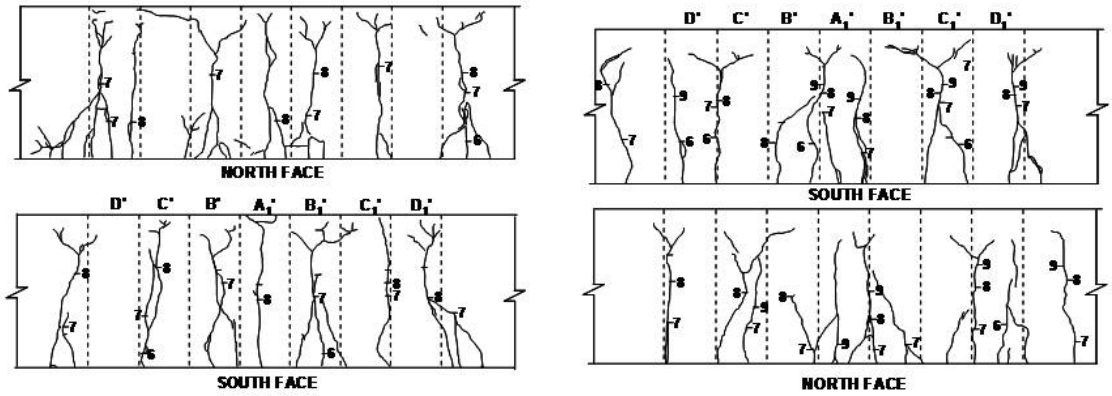

Beam B2-1 Beam B3-1

Fig. 10 Observed crack pattern for beams B2-1 and B3-1 (numbers denote the loading stage)

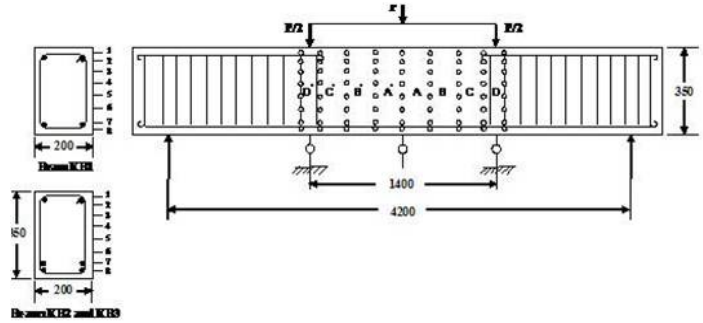

Fig. 11 Schematic representation of test program (Desayi and Rao 1987, 1989) (dimensions in mm)

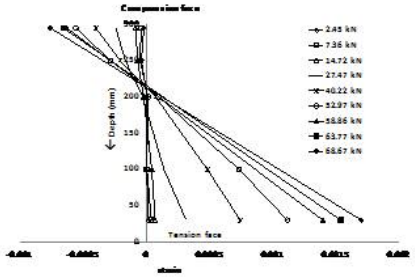

Fig. 12 Strain variation across the depth for different stages of loading for beam B2-2

7.2 Experimental investigations presented by Desayi and Rao (1987, 1989)

Three beams of similar cross-sectional dimensions of 250 mm x 350 mm and 4.8 m long were cast and tested in two-point bending over an effective span of 4.2 m. Stirrups of 6 mm diameter were provided in the combined bending and shear zone to avoid shear failure, and no stirrups were provided in the constant bending moment zone. Details of the beams are given in Table 3. The constant bending moment zone of the beams (1.4 m) was divided into eight sections (denoted as D', C', B', A', A, B, C and D on the west face and, D_1, C_1, B_1, A_1, A_1', B_1', C_1' and D_1' on the east face),

with each section having a gauge length 200 mm (see Fig. 11). In each section, demec points were fixed at eight different positions on both faces of the beam (east face and west face). As can be seen from Fig. 11, position 1 corresponds almost to the extreme compression fibre for all beams; and position 7 in case of beam KB1 and positions 7 and 8 in case of beams KB2 and KB3 correspond to position of steel bars. The beams were tested in two-point loading in a 25 ton (245.25 kN) capacity testing frame. To measure the surface strains at different positions, a demec gauge with least count $1x10^{-5}$ and gage length of 200.1 mm was used. The loads applied on the beams at different loading stages are given in Table 4.

8. Statistical analysis of strain

Only the strains measured at the level of tension reinforcement is considered further in the analysis.

8.1 Statistical modeling of strains for the beams tested at CSIR-SERC

In the present study, the aim is to model the strain in concrete at the level of bottom layer of main reinforcement (position 5 in Fig. 4) for a given loading stage. Three loading stages are considered for the sets B2 and B3, namely those corresponding to applied loads of 27.47 kN, 40.22 kN and 52.97 kN. It is known that evaluation of performance of reinforced concrete structural members under service loads is important in service life estimation. By defining the service load as approximately two-thirds of ultimate load, it is noted that the applied loads corresponding to the three loading stages considered in this study are less than the service loads, thereby helping in understanding the strain behavior of flexural members under normal working load conditions. The typical variation of average strain across the depth for different stages of loading for the beam B2-2 is shown in Fig. 12. It is noted that the strain variation across the depth is almost linear for the loading stages considered in the present study. Similar observation is made for the other three beams also; however, the results are not presented here. This is in line with the observation regarding strain variation across the depth made by Neild *et al.* (2002).

At any given loading stage, fourteen strain readings (seven on the north face and seven on the south face) in the constant bending moment region are available for each beam in the sets B2 and B3. To enhance the sample size, the strain readings, corresponding to the same applied load, of both the beams in each set are combined together. This can be justified since the ultimate loads, cube compressive strengths and split tensile strengths for the two beams in each set are comparable with each other (see Table 2). It is also noted that the depth of neutral axis (determined using the strain gauge readings at different positions) at different loading stages for the two beams in each set are comparable, except for set B2 at an applied load of 27.47 kN. After combining the respective strain readings of beams belonging to sets B2 and B3, there are twenty-eight strain readings, at any given loading stage. These values are further processed for modeling the random variations in strain in concrete (at the level of reinforcement).

8.2 Statistical modeling of strains for the beams presented by Desayi and Rao (1987, 1989)

At any given loading stage, sixteen strain readings (eight on the west face and eight on the east

face) in the constant bending moment region are available for the beams KB1, KB2 and KB3. These values are further processed for modeling the random variations in strain in concrete at the level of reinforcement (position 7 in case of beam KB1 and position 8 in case of beams KB2 and KB3).

Table 5 Statistical properties of observed strains (based on tests conducted) and parameters of alpha-stable distribution of strain

Beam	Applied Load (kN)	Statistical properties of experimentally observed strains			Parameters of α-stable distribution for strain			
		Mean	SD	Skewness	α	β	c	δ
B2	27.47	0.000264	0.000276	0.0738	1.9363	1.0	0.000215	0.000271
	40.22	0.000716	0.000626	-0.3208	1.2027	-1.0	0.000402	-0.00016
	52.97	0.001145	0.000847	-0.7273	0.97	-0.721	0.000408	0.00779
B3	27.47	0.000365	0.000280	0.3847	1.5828	1	0.000213	0.00044
	40.22	0.000911	0.000585	-0.2716	1.5395	-1	0.00044	0.00072
	52.97	0.001343	0.000959	-0.3025	1.5142	-1	0.000704	0.00102
KB1	10.52	0.000057	0.000017	0.7689	1.2440	0.5040	0.000010	0.000065
	16.61	0.000106	0.000034	0.4319	1.3954	0.9990	0.000024	0.000125
	28.99	0.000499	0.000205	0.0401	1.4181	0.0687	0.000146	0.000505
	38.28	0.000878	0.000355	-0.0373	1.6004	0.2121	0.000260	0.000900
	48.95	0.001252	0.000478	-0.0720	1.1038	0.1880	0.000282	0.001536
	57.37	**0.001529**	**0.000555**	**-0.0637**	**1.0412**	**0.1133**	**0.000300**	**0.002030**
	65.66	**0.001871**	**0.000645**	**-0.064**	**0.9001**	**0.0446**	**0.000319**	**0.001775**
KB2	4.48	0.000036	0.000018	1.8463	1.4839	0.999	0.000010	0.000039
	8.90	0.000075	0.000029	1.1304	1.4459	0.4437	0.000017	0.000078
	14.24	0.000131	0.000033	-0.1281	1.3705	-0.425	0.000020	0.000123
	17.80	0.000220	0.000079	0.4800	0.6429	-0.042	0.000025	0.000217
	22.25	0.000440	0.000108	0.1806	2.000	0.1107	0.000091	0.000438
	26.67	0.000724	0.000182	0.2818	1.0931	0.3391	0.000112	0.000942
	35.42	0.001150	0.000327	0.0842	1.3881	0.2244	0.000234	0.001195
	44.16	**0.001521**	**0.000455**	**0.0199**	**1.1381**	**0.2552**	**0.000294**	**0.001799**
	57.44	**0.002693**	**0.000929**	**0.4189**	**0.9001**	**0.0446**	**0.000319**	**0.001775**
KB3	8.90	0.000079	2.74E-05	-0.8468	1.1794	-0.221	0.000017	0.000071
	17.80	0.000296	0.000091	0.9445	1.4134	0.999	0.000056	0.000332
	26.67	0.000741	0.000249	0.3524	1.7428	0.999	0.000206	0.000776
	39.78	0.001379	0.000420	-0.2309	1.8903	-0.999	0.000370	0.001359
	52.97	0.002069	0.000644	-0.3139	1.828	-0.999	0.000555	0.002014
	70.90	**0.006603**	**0.002394**	**-0.0091**	**1.9997**	**0.9988**	**0.002276**	**0.006595**

(Note: Values in bold face indicate the loading stages where no new cracks are formed (stabilized crack growth), Values in shaded cells represent departures from the expected trend, which may be due to anomalies in experimentation during that loading stage)

9. Results and discussion

The statistical properties (namely, mean, standard deviation and skewness) of the strain in concrete at the level of reinforcement have been computed based on the observed strain values. An alpha-stable distribution, $S(\alpha, \beta, c, \delta)$ is fitted to the strains in concrete at the level of reinforcement at each loading stage for the beams considered. The parameters α, β, c and δ of the alpha-stable distribution (Eq. (6)) are estimated using an optimization procedure by minimizing the sum of squares of the difference between the observed cumulative distribution function (empirical distribution function) and the cumulative distribution function (CDF) of the alpha-stable distribution.

9.1 Beams Tested at CSIR-SERC

The parameters of the alpha-stable distribution of strain for sets B2 and B3 for the applied loads considered are given in Table 5. The variation in characteristic exponent, α, with applied load is shown in Fig. 13. It is noted that the values of α decreases with increase in applied load for both B2 and B3. It is known that for α=2, the alpha-stable distribution becomes normal distribution, and as α reduces, the tails get heavier, i.e., the tail probabilities increase (Nolan 2009). This indicates that at higher stages of loading, the strain distribution deviates away from the normal distribution. This can be attributed to the formation of emergent structures and associated strain redistributions in concrete as explained in the section on mechanism of cracking. It is also noted from Fig. 13 that the reduction in α is much higher in set B2 when compared to set B3. This may be because in set B3, the cracks are more evenly distributed (lower values of crack spacing which can be attributed to the more number of smaller diameter reinforcing bars in the beams in set B3 when compared to beams in set B2, with total area of steel in tension zone remaining approximately the same), and hence the variability in strain are less, leading to lower values of tail probabilities.

The probability density functions (PDFs) and cumulative distribution functions (CDFs) of strain for the sets B2 and B3 at different applied loads considered are shown in Fig. 14. From these figures, it is noted that the distribution of strain changes from right-skewed (for applied load of 27.47 kN) to left-skewed with increase in loading. It is noted that, as expected the peak of the distribution shifts to the right, along with an increase in the spread of the distribution, with increase in applied load. This suggests that a fat-tailed distribution need to be used at these stages

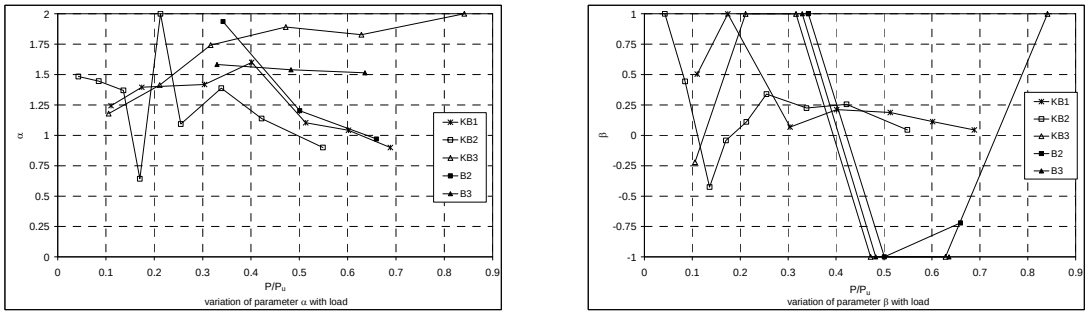

Fig. 13 Variation in parameters α and β with applied load

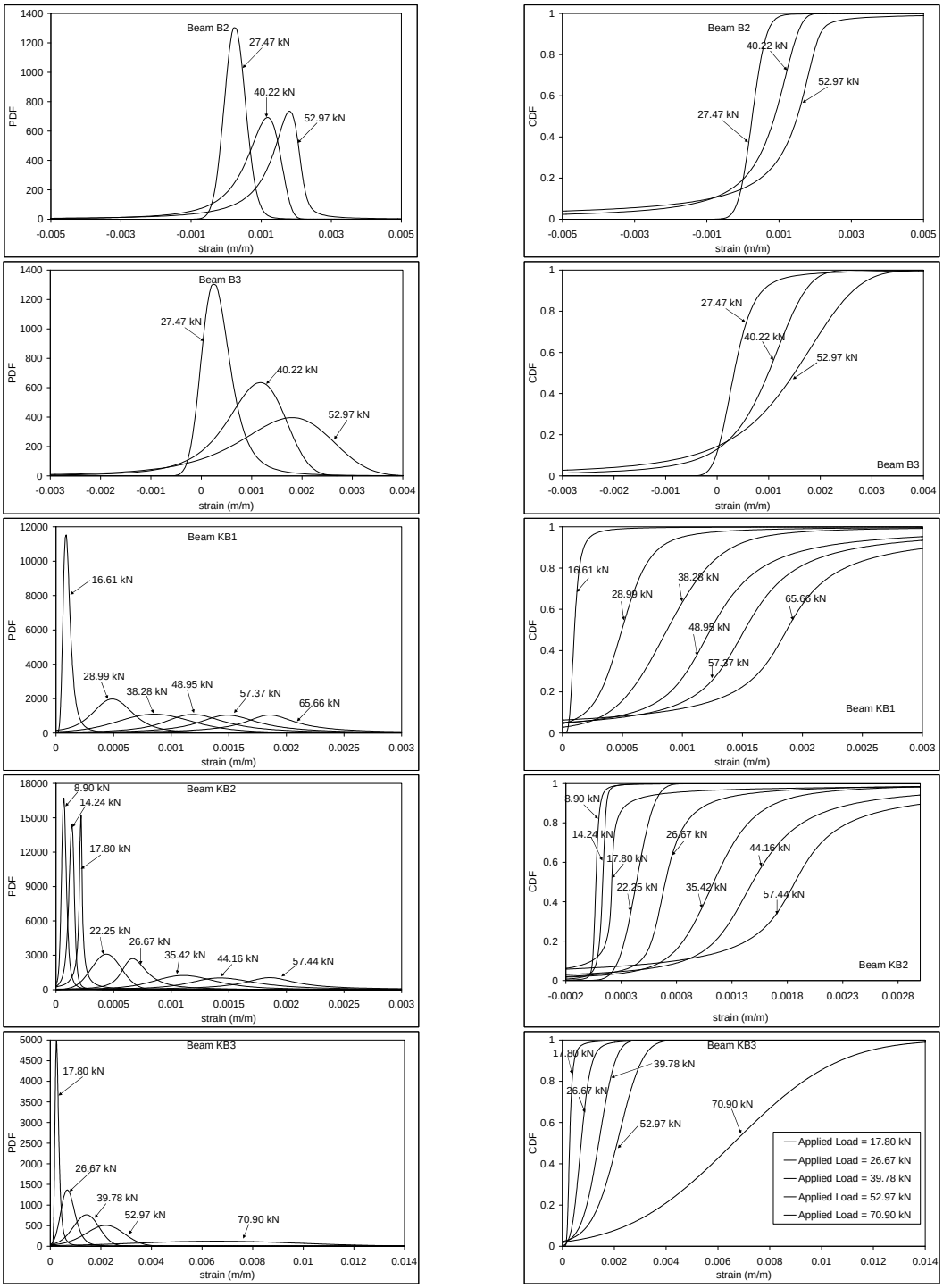

Fig. 14 PDFs and CDFs of alpha-stable distributions of strain for different values of applied load for the beams considered

of loading.

From Fig. 13, it is noted that the value of the stability parameter (α) is almost a constant for set B3, while it shows large variation for set B2. This indicates that the strain distribution is almost stabilized for set B3. Since the strains in concrete in the tension depends on the level of cracking, a stabilized strain distribution suggests that the cracking has stabilized, i.e., no new cracks are being formed with increase in loading, rather the existing cracks are widened and extended. This is also supported by the observed crack patterns for the beams in set B3 (see Fig. 10), from which it is noted that no new major cracks are formed after the loading stage 7 (corresponding to applied load of 40.22 kN). However, from the observed crack pattern for a beam in set B2 (see Fig. 10), it is noted that a major crack has formed at the loading stage 8 (corresponding to applied load of 52.97 kN). This shows that the cracking and hence the strain distribution has not stabilized for set B2. This trend is also reflected in the values of the scale parameter (c) and the location parameter (δ) given in Table 5. The values of c and δ increase with applied load when the strain distribution is stabilized (as is the case for set B3), indicating that the strains are increasing at an almost uniform rate in all the sections. However, when new cracks form (as is the case for set B2), there is sudden increase of strain in the section containing the crack, and a decrease in strain in the adjacent sections, leading to abrupt variations in c and δ.

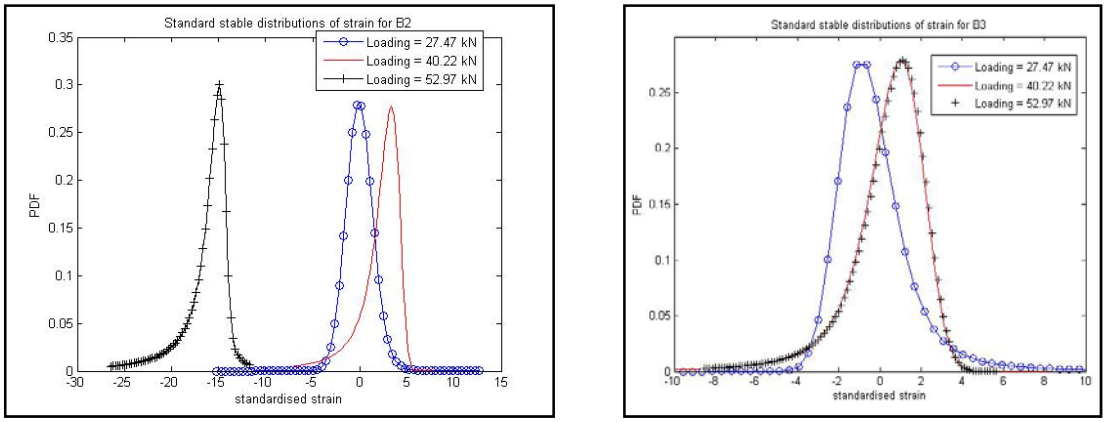

Fig. 15 Standardized alpha-stable distributions of strain for sets B2 and B3

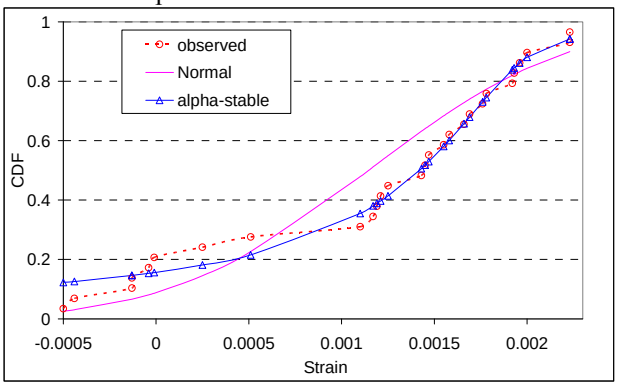

Fig. 16 Comparison of CDFs of strain for set B2 (applied load = 52.97 kN)

The standardized alpha-stable distributions of strains, for sets B2 and B3, for the applied loads considered are determined using Eq. (7) and are shown in Fig. 15, respectively. For set B2, the standardized alpha-stable distributions for different applied loads are quite distinct, indicating that the cracking is not stabilized. However, for set B3, the standardized alpha-stable distributions for applied loads of 40.22 kN and 52.97 kN are almost identical, indicating that the cracking has stabilized at the applied load of 40.22 kN, which is also noted from the experimentally observed crack pattern. The stabilization of cracking for set B3 also reinforces the guidelines given in literature that it is better to use more number of smaller diameter bars for control of cracking in reinforced concrete flexural members.

For the purpose of comparison, a normal distribution is also fitted to the observed strain data (by considering the mean and standard deviation of the normal distribution as the average and standard deviation of the observed strain data). The observed CDF, alpha-stable CDF and the normal CDF, typically for the set B2, for an applied load of 52.97 kN, are shown in Fig. 16. From this figure, it is noted that CDF corresponding to the alpha-stable distribution compares with the observed CDF better than the normal CDF (especially in the tail regions which is of interest in estimating extreme values of strains).

9.2 Beams presented by Desayi and Rao (1987, 1989)

The parameters of the alpha-stable distribution of strain for the beams KB1, KB2 and KB3 for the applied loads considered are given in Table 5. The variations in α and β with applied load are shown in Fig. 13. For the beam KB3, which has well distributed reinforcement, it is noted that α values increase with loading and reaches a value of 2.0. For the beams KB1 and KB2, with increase in load, the values of α moves closer to 1.0. These observations suggest that the strain localization effects may not be significant if the density of cracking is higher (as is the case for the beam KB3). In such cases, it can be assumed that the surface strains follow normal distribution at higher stages of loading. It is noted from Table 5 that, in general, the trends of skewness of the fitted alpha-stable distribution are in agreement with the trends of skewness shown by the measured strain readings, which indicate the ability of the fitted alpha-stable distribution to represent the measured variations in strain. For the beams KB1 and KB2, the general tendency for β is to decrease with the increase in loading. In the case of beam KB3, α values are close to 2 and hence β does not have any meaning. Therefore, when the density of cracking is less (i.e., when

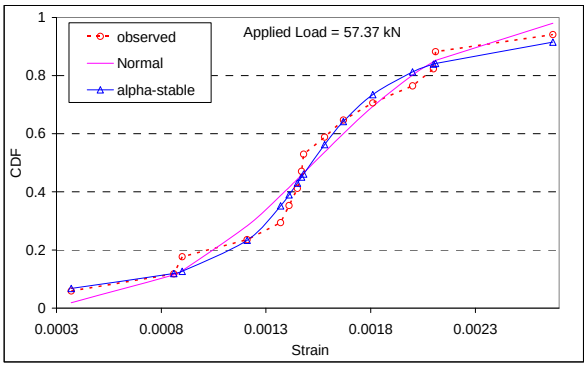

Fig. 17 Comparison of CDFs of strain for beam KB1 (applied load = 57.37 kN)

cracks are widely spaced apart), an alpha stable distribution with small value of asymmetry parameter is desirable to describe the fluctuations in surface strains. The probability density functions (PDFs) and cumulative distribution functions (CDFs) of alpha-stable distribution of strain are shown in Fig. 14. From Fig. 14, it is noted that the PDFs of strain are highly peaked for loading stages corresponding to uncracked/low levels of cracking. As the level of cracking increases, the PDFs of strain become more and more flat, justifying the use of alpha-stable distributions. The observed CDF, alpha-stable CDF and the normal CDF, typically for the beam KB1, for an applied load of 57.37 kN, are shown in Fig. 17. From Fig. 17, it is noted that CDF corresponding to the alpha-stable distribution compares with the observed CDF better than the normal CDF. This observation suggests that alpha-stable distribution is a better fit to the observed strain readings (especially in the tail regions which is of interest in estimating extreme values of strains).

9.3 General observations

Of the four parameters of the alpha-stable distribution, namely, α, β, c and δ, the characteristic exponent α is the most important parameter. From the variation in α with applied load (see Fig. 13) for the beams considered, it is noted that, in general, for beams with lesser specific surface area (or perimeter) for a given cross-sectional area of steel, α becomes close to 1.0 when the cracking has stabilized (i.e., no new cracks are formed). An assumption of a value of $\alpha = 2.0$ for beams with well distributed bars for the same cross-sectional area of steel is more appropriate. The value of α decides the probability content in the tail portions of the probability distribution, and as α reduces, the probability distribution become more and more heavy-tailed (and deviates more and more from the normal distribution). These observations indicate that when we are trying to model the probabilistic variations or choose a probability density function of surface strain for beams with lesser perimeter of reinforcement, use of alpha-stable distribution become important.

As noted earlier, the skewness parameter β is not the same as the classical skewness parameter (Nolan 2009), since for non-Gaussian stable distributions, the moments do not exist. It is noted that the trends of skewness of the fitted alpha-stable distribution are in agreement with the trends of skewness shown by the observed strain readings. This observation also suggests the ability of the fitted alpha-stable distribution to represent the observed variations in strain.

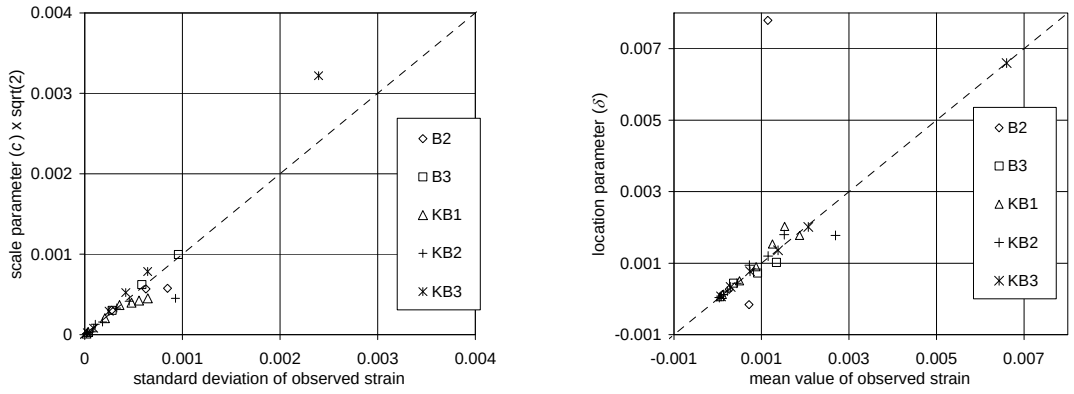

Fig. 18 Comparison of $c\times\sqrt{2}$ and δ with the standard deviation- and mean- of measured strain values

The scale parameter c is a measure of width of the probability distribution (Borak *et al.* 2005). For $\alpha = 2$, the value of standard deviation = $c \times \sqrt{2}$. The values of standard deviation computed based on observed strain values are compared with the values of $c \times \sqrt{2}$ in Fig. 18. It is noted that values of $c \times \sqrt{2}$ are comparable with the computed values of standard deviation (even though the standard deviation does not exist for alpha-stable distribution when $\alpha < 2$). This observation suggests that while fitting the alpha-stable distribution (using the methodology presented in Fig. 9), the initial guess value of c for the optimization can be estimated from the experimentally observed or numerically determined standard deviation of surface strain.

The location parameter δ is the mode (peak) of the alpha-stable distribution (Borak *et al.* 2005). From Fig. 13, it is noted that for the beams, at almost all stages of loading, the α values are greater than 1.0, which indicates that the mean exists. The values of average surface strain computed based on observed strain values are compared with the values of δ in Fig. 18. It is noted that values of δ are in good agreement with the computed values of average strain (except for beam B2). This observation suggests that the location parameter δ can be estimated from the experimentally observed or numerically determined mean values of surface strain.

The investigations reported in this paper will help in describing the appropriate probability distribution for surface strain at the level of steel while carrying out probabilistic response analysis of reinforced concrete flexural beams using numerical methods. Further investigations are required to be carried out for determining the appropriate type of probability distributions for other failure mechanisms. For plain concrete elements in tension, it has been reported that the probability distribution can be described using KLE techniques (Ibrahimbegovic 2011, Benkemoun 2010). However, the use of KLE is basically for Gaussian random fields. For alpha-stable random fields, which arise in the case of reinforced concrete, the applicability of polynomial chaos expansion can be explored (Xiu and Karniadakis 2002). However, for beams with well distributed reinforcement in the tension zone (for instance, KB3), the α values become closer to 2 (with increase in applied load), suggesting a normal distribution for surface strain. In such cases, the use of KLE for describing the probability distribution can be explored. However, this is not in the scope of the present investigation, and any theoretical/numerical modeling is not attempted.

10. Conclusions

Based on phenomenological, thermodynamic and statistical considerations, alpha-stable distributions) are proposed for modeling the variations in strain in reinforced concrete flexural members to account for the large fluctuations. Applicability of alpha-stable distributions is examined using experimentally obtained strain values from reinforced concrete flexural members tested under four-point bending. From the results obtained, it is noted that alpha-stable distribution is a better fit to the observed strain readings at a given stage of loading, than the normal distribution, especially in the tail regions which is of interest in estimating extreme values of strains. While estimation of parameters of alpha-stable distributions is still an active area of research, the initial studies presented in this paper shows promise regarding the usefulness these distributions. Since the data from the experimental instigations are limited, there is a need to conduct further independent finite element simulation studies using the appropriate models based on thermodynamics considerations (such as the strong discontinuity model proposed by Dominguez *et al.* (2005) and furthered in Ibrahimbegovic *et al.* (2010)) for cracking of concrete.

Acknowledgments

This paper is being published with the kind permission of Director, CSIR-Structural Engineering Research Centre, Chennai, India. The authors are thankful to Mr. Kumarappan, Technical Officer, Structural Testing Laboratory, CSIR-SERC, for his unstinting help in carrying out the experimental work. The MATLAB programs developed by Mark Veillette, Ph.D. Scholar, Department of Mathematics and Statistics, Boston University, Boston, USA, have been used in the present study for determining the CDFs and PDFs of the alpha-stable distributions.

References

ACI (2002), *Control of cracking in concrete structures*, ACI manual of concrete practice, ACI 224, American Concrete Institute, Detroit.

Balaji Rao, K. and Appa Rao, T.V.S.R. (1999), "Cracking in reinforced concrete flexural members - a Reliability Model", *Struct. Eng. Mech*., **7**(3), 303-318.

Balaji Rao, K. (2009), "The applied load, configuration and fluctuation in non-linear analysis of reinforced concrete structures - some issues related to performance based design", *Proceedings of International Conference on Advances in Concrete, Structural and Geotechnical Engineering (ACSGE 2009)*, BITS Pilani, India.

Bates, S. and McLaughlin, S. (2000), "The estimation of stable distribution parameters from teletraffic data", *IEEE T. Signal Proces*., **48**(3), 865-870.

Bazant, Z.P. (2002), *Scaling of structural strength*, Elsevier Butterworth-Heinemann, Second Edition.

Bazant, Z.P. and Cedolin, L. (2010), *Stability of structures - elastic, inelastic, fracture and damage theories*, World Scientific.

Bazant, Z.P. and Oh, B.H. (1983), "Spacing of cracks in reinforced concrete", *J. Struct. Eng.-ASCE*, **109**(9), 2066-2085.

Belov, I.A. (2005), "On the computation of the probability density function of-stable distributions", *Math. Model. Anal. Proc. 10th International Conference MMA2005&CMAM2*, Trakai. 333-341.

Benkemoun, N., Hautefeuille, M., Colliat, J.B. and Ibrahimbegovic, A. (2010), "Failure of heterogeneous materials: 3D meso-scale FE models with embedded discontinuities", *Int. J. Numer. Meth. Eng*., **82**(13), 1671-1688.

Borak, S., Härdle, W. and Weron, R. (2005), "Stable distributions", SFB 649 Discussion Paper 2005-008, SFB 649, Humboldt-Universitä zu Berlin.

Bresler, B. (1974), *Reinforced concrete engineering: Vol.1-materials, structural elements, safety*, John Wiley and Sons, New York.

BS 8110 (1997), *Structural use of concrete*, Code of Practice for Design and Construction, British Standards Institution, UK

Carpinteri, A. and Puzzi, S. (2009), "The fractal-statistical approach to the size-scale effects on material strength and toughness", *Probab. Eng. Mech*., **24**(1), 75-83.

Carpinteri, A., Cornetti, P. and Puzzi, S. (2006), "Scaling laws and multiscale approach in the mechanics of heterogeneous and disordered materials", *Appl. Mech. Rev*., **59**(5), 283-305.

CEB (1990), *Model code for concrete structures*, Euro-International Concrete Committee, Switzerland.

de Borst, R. (1987), "Computation of post-buckling and post-failure behavior of strain-softening solids", *Comput. Struct*., **25**(2), 211-224.

de Borst, R., Gutierrez, M.A., Wells, G.N., Remmers, J.J.C and Askes, H. (2004), "Cohesive-zone models, higher-order continuum theories and reliability methods for computational failure analysis", *Int. J. Numer. Meth. Eng*., **60**, 289-315.

de Groot, S.R. and Mazur, P. (1984), *Non-equilibrium thermodynamics*, Dover Publications.

Desayi, P and Rao, B.K. (1987), "Probabilistic analysis of cracking of RC beams", *Mater. Struct*., **20**(120), 408-417.
Desayi, P. and Rao, B.K. (1989), "Reliability of reinforced concrete beams in limit state of cracking - failure rate analysis approach", *Mater. Struct*., **22**(4), 269-279.
Desayi, P. and Ganesan, N. (1985), "An investigation on spacing of cracks and maximum crackwidth in reinforced concrete flexural members", *Mater. Struct*., **18**(104), 123-133.
Dominguez, N., Brancherie, D., Davenne, L. and Ibrahimbegovic, A. (2005), "Prediction of crack pattern distribution in reinforced concrete by coupling a strong discontinuity model of concrete cracking and a bond-slip of reinforcement model", *Int. J. Comput. Aid. Eng. Softw*., **22**(5-6), 558-582.
Fama, E.F. and Roll, R. (1968), "Some properties of symmetric stable distributions", *J. Am. Stat. Assoc*., **63**(323), 817-836.
Ibrahimbegovic, A., Boulkertous, A., Davenne, L. and Brancherie, D. (2010), "Modelling of reinforced-concrete structures providing crack-spacing based on X-FEM, ED-FEM and novel operator split solution procedure", *Int. J. Numer. Meth. Eng*., **83**, 452-481.
Ibrahimbegovic, A., Colliat, J.B., Hautefeuille, M., Brancherie, D. and Melnyk, S. (2011), "Probability based size effect representation for failure of civil engineering structures built of heterogeneous materials", *Comput. Meth. Stoch. Dyn*., **22**, 289-311.
Kogon, S.M. and Williams, D.B. (1995), "On the characterization of impulsive noise with alpha-stable distributions using fourier techniques", *29th Asilomar Conf. Signals, Syst. Comput*.
Koutrouvelis, I.A. (1980), "Regression-type estimation of the parameters of stable laws", *J. Am. Stat. Assoc*., **75**(372), 918-928.
Ma, X. and Nikias, C.L. (1995), "Parameter estimation and blind channel identification in impulsive signal environments", *IEEE T. Signal Proces*., **43**(12), 2884-2897.
MacGregor, J.G. (1997), *Reinforced concrete: Mechanics and design*, Third Edition, Prentice Hall Inc., New Jersey.
Maymon, S., Friedmann, J. and Messer, H. (2000), "A new method for estimating parameters of a skewed alpha-stable distribution", *Proceedings of the Acoustics, Speech, and Signal Processing 2000 (ICASSP '00)*, IEEE International Conference, **6**, 3822-3825.
Mandelbrot, B. and Taleb, N. (2006), "A focus on the exceptions that prove the rule", Financial Times.
McCulloch, J.H. (1986), "Simple consistent estimators of stable distribution parameter", *Commun. Stat.-Simul*., **15**(4), 1109-1136.
Neild, S.A., Williams, M.S. and McFadden, P.D. (2002), "Non-linear behaviour of reinforced concrete beams under low-amplitude cyclic and vibration loads", *Eng. Struct*., **24**(6), 707-718.
Nilson, A.H and Winter, G. (1986), *Design of concrete structures*, Tenth Edition, McGraw-Hill Book Company, New York.
Nolan, J.P. (2009), *Stable distributions: Models for heavy tailed data*, Boston: BirkhÄauser, Unfinished manuscript, Chapter 1 online at academic2.american.edu/»jpnolan.
Park, R. and Paulay, T. (1975), *Reinforced concrete structures*, John Wiley and Sons, A Wiley-InterScience Publication, New York.
Pillai, U. and Menon, D. (2009), *Reinforced concrete design*, Third edition, Tata McGraw-Hill, New Delhi.
Prigogine, I. (1967), *Introduction to thermodynamics of irreversible processes*, Third Edition, Interscience Publishers, New York.
Prigogine, I. (1978), "Time, structure, and fluctuations", *Sci*., **201**(4358), 777-785.
Rubi, J.M. (2008), "The long arm of the second law", Scientific American, 62-67.
Sluys, L.J. and de Borst, R. (1996), "Failure in plain and reinforced concrete – an analysis of crack width and crack spacing", *Int. J. Solid. Struct*., **33**(20-22), 3257-3276.
Tsihrintzis, G.A. and Nikias, C.L. (1996), "Fast estimation of the parameters of alpha-stable impulsive interference", *IEEE T. Signal Proces*., **44**(6), 1492-1503.
Xiu, D. and Karniadakis, G.E. (2002), "The wiener-askey polynomial chaos for stochastic differential equations", *SIAM J. Sci. Comput*., **24**(2), 619-644.
Yang, C.Y., Hsu, K.C. and Chen, K.C. (2009), "The use of the levy-stable distribution for geophysical data

analysis", *Hydrogeol. J*., 17:1265-1273.

CC

Appendix I

The application of non-equilibrium thermodynamics helps in accounting for: (1) irreversibility in evolution, (2) the complexity generation (viz., cracking) and (3) self-organising behavior at the points of instability (characterized by probability density functions with power law decaying tails). A diagrammatic representation of evolution of such a system is shown in Fig. A-1. As the internal order within the system becomes complex, the system is no longer able to remain organized and becomes unstable. This instability within the system stimulates a bifurcation event that leads to new states of order because both descendent branches have less entropy than the ancestral branch. At the point of bifurcation, maximum uncertainty exists as to which path to take. Once a path is chosen, it will evolve such that internal entropy production is minimized. In this description, the system can be considered as the reinforced concrete beam, and the source of energy is the external loading system.

Appendix II

A probability density $L(x)$ can be a limiting distribution of the sum $\sum_{i=1}^{\infty} X_i$ of independent and randomly distributed variables only if it is stable. A random variable X is stable or stable in the broad sense if for X_1 and X_2 independent copies of X and any positive constants a and b

$$a X_1 + b X_2 \overset{d}{=} c X + d \tag{A.1}$$

holds for some positive c and some $d \in \Re$ (Nolan, 2009). The symbol $\overset{d}{=}$ means equality in distribution, i.e., both the expressions have the same probability law. The term stable is used because the shape is stable or unchanged under sums of the type given by Eq. (A.1).

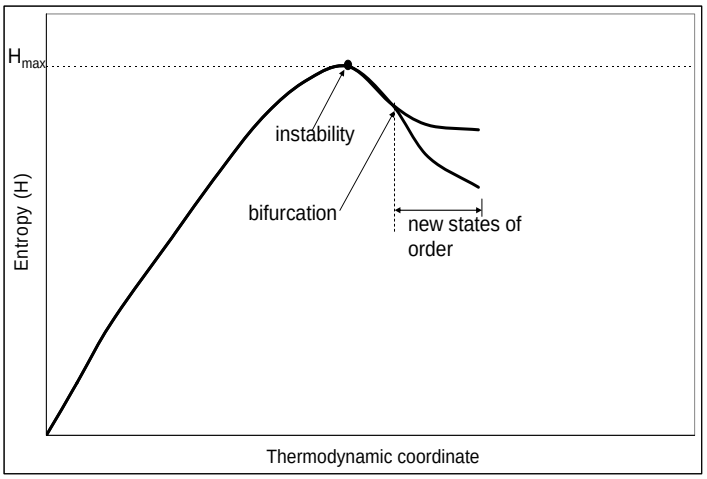

Fig. A-1 Diagrammatic representation of evolution of a non-equilibrium thermodynamic system

The Gaussian- and Cauchy- distributions are potential limiting distributions, depending on the physical phenomenon that is being handled. However, there are many more distributions to which the summation series $\sum_{i=1}^{\infty} X_i$ is attracted to depending on the actual behaviour. The complete set of stable distributions have been specified by Levy and Khinchine. A probability distribution is stable if its characteristic function is of the form as given in Eq. (6).

While Eq. (6) defines the general expression for all possible stable distributions, it does not specify the conditions which the probability density function (pdf) $p(l)$ has to satisfy so that the distribution of the normalized sum $\hat{S}_n = \sum_{i=1}^{n} p_i(l)$ converges to a particular $L_{\alpha,\beta}(x)$ in the limit $n \to \infty$. If this is the case, one can say ' $p(l)$ belongs to the domain of attraction of $L_{\alpha,\beta}(x)$'. This problem has been solved completely and the answer can be summarized by the following theorem.

Theorem: The probability density $p(l)$ belongs to the domain of attraction of a stable density $L_{\alpha,\beta}(x)$ with characteristic exponent α ($\alpha \in (0 < \alpha < 2)$) iff

$$p(l) \sim \frac{\alpha a^{\alpha} c_{\pm}}{|l|^{1+\alpha}} \quad \text{for} \quad l \to \pm\infty \tag{A.2}$$

where $c_+ \geq 0$, $c_- \geq 0$ and a are constants. These constants are directly related to the scale parameter c and the skewness parameter β by

$$c = \begin{cases} \dfrac{\pi(c_+ + c_-)}{2\alpha\Gamma(\alpha)\sin(\pi\alpha/2)} & \text{for } \alpha \neq 1 \\ \dfrac{\pi}{2}(c_+ + c_-) & \text{for } \alpha = 1 \end{cases} \tag{A.3}$$

$$\beta = \begin{cases} \dfrac{c_- - c_+}{c_+ + c_-} & \text{for } \alpha \neq 1 \\ \dfrac{c_+ - c_-}{c_+ + c_-} & \text{for } \alpha = 1 \end{cases} \tag{A.4}$$

Furthermore, if $p(l)$ belongs to the domain of attraction of a stable distribution, its absolute moments of order λ exists for $\lambda < \alpha$.

$$\left\langle |l|^{\lambda} \right\rangle = \int_{-\infty}^{\infty} dl\, |l|^{\lambda}\ p(l) = \begin{cases} < \infty & \text{for } 0 \leq \lambda \leq \alpha\,(\alpha \leq 2) \\ \infty & \text{for } \lambda > \alpha\,(\alpha < 2) \end{cases} \tag{A.5}$$

The above discussion clearly brings out that the sum of independent random variables, as $n \to \infty$, may converge to an alpha-stable distribution, $\alpha = 2$ being a specific case, with $p(l) \sim 1/|l|^3$, as a Gaussian distribution. For all other values of characteristic exponent, α,

$0 < \alpha < 2$, the sum would be attracted to $L_{\alpha,\beta}(x)$ and all these classes of stable distributions show the same asymptotic behaviour for large *x*. Thus, the central limit theorem can be generalized as follows:

The generalised central limit theorem states that the sum of a number of random variables with power-law tail distributions decreasing as $1/|x|^{\alpha+1}$ where $0 < \alpha < 2$ (and therefore having infinite variance) will tend to a stable distribution as the number of variables grows.

The characteristic exponent α and the skewness (symmetry) parameter β have to be interpreted based on physical significance. As already mentioned, α defines the shape of the distribution and decides the order of moments available for a random variable. Longer power-law tails will lead to divergence of even lower order moments. This should not be treated as a limitation, since, in some of the physical systems, the pdf of response quantities can have power-law tails. This may also be true of nonlinear response of engineering systems, especially at bifurcation points, where the system can exhibit longer tail behaviour. Though this can be brushed aside as a transient behaviour, for seeking performance of a system, this needs to be effectively handled. Hence, it is important to understand the pdfs and associated properties, so that the systems can be modeled realistically.